EPA-R4-73-030e

July 1973

ENVIRONMENTAL MONITORING SERIES

URBAN AIR SHED PHOTOCHEMICAL SIMULATION MODEL STUDY

VOLUME I - DEVELOPMENT AND EVALUATION

Appendix D - Numerical Integration of Continuity Equations

Office of Research and Development
U.S. Environmental Protection Agency
Washington, D.C. 20460

EPA-R4-73-030e

URBAN AIR SHED PHOTOCHEMICAL SIMULATION MODEL STUDY

VOLUME I - DEVELOPMENT AND EVALUATION

Appendix D - Numerical Integration of Continuity Equations

by

S. D. Reynolds

Systems Applications, Inc.
9418 Wilshire Boulevard
Beverly Hills, California 90212

Contract No. 68-02-0339
Program Element No. 1A1009

EPA Project Officer: Herbert Viebrock

Meteorology Laboratory
National Environmental Research Center
Research Triangle Park, North Carolina 27711

Prepared for

OFFICE OF RESEARCH AND DEVELOPMENT
U.S. ENVIRONMENTAL PROTECTION AGENCY
WASHINGTON, D.C. 20460

July 1973

This report has been reviewed by the Environmental Protection Agency and approved for publication. Approval does not signify that the contents necessarily reflect the views and policies of the Agency, nor does mention of trade names or commercial products constitute endorsement or recommendation for use.

EPA-R4-73-030e

URBAN AIR SHED PHOTOCHEMICAL SIMULATION MODEL STUDY

VOLUME I - DEVELOPMENT AND EVALUATION

Appendix D - Numerical Integration of Continuity Equations

by

S. D. Reynolds

Systems Applications, Inc.
9418 Wilshire Boulevard
Beverly Hills, California 90212

Contract No. 68-02-0339
Program Element No. 1A1009

EPA Project Officer: Herbert Viebrock

Meteorology Laboratory
National Environmental Research Center
Research Triangle Park, North Carolina 27711

Prepared for

OFFICE OF RESEARCH AND DEVELOPMENT
U.S. ENVIRONMENTAL PROTECTION AGENCY
WASHINGTON, D.C. 20460

July 1973

This report has been reviewed by the Environmental Protection Agency and approved for publication. Approval does not signify that the contents necessarily reflect the views and policies of the Agency, nor does mention of trade names or commercial products constitute endorsement or recommendation for use.

TABLE OF CONTENTS

		Page
INTRODUCTION		D-1
I.	THE METHOD OF FRACTIONAL STEPS APPLIED TO THE INTEGRATION OF THE MASS CONSERVATION EQUATIONS	D-6
	A. Transformation of the Governing Equations	D-6
	B. The Computational Grid	D-11
	C. Nomenclature	D-11
	D. Finite-Difference Equations	D-13
II.	METHODS FOR SOLVING THE LINEAR SYSTEMS OF EQUATIONS	D-33
	A. The Algorithm for the Tridiagonal System	D-34
	B. The Algorithm for the Block-Tridiagonal System	D-35
III.	DISCUSSION OF THE NUMERICAL METHOD	D-38

INTRODUCTION

In this Appendix we present a comprehensive discussion of the methodology used to obtain the numerical solution of the governing airshed equations. During this second phase of model development and evaluation, we have carried out further studies of the numerical scheme described in Appendix D of Roth et al. (1971) and implemented several important changes. We shall discuss the motivation for making these changes and include a complete description of the finite-difference equations that were finally adopted. All simulation results included in the Final Report were obtained using the numerical methods described in Sections I and II.

We begin by writing the governing airshed equations, which express the conservation of mass of each chemical species in a turbulent fluid in which chemical reactions occur. Employing the so-called K-theory, these equations can be written as:

$$\frac{\partial c_\ell}{\partial t} + \frac{\partial u c_\ell}{\partial x} + \frac{\partial v c_\ell}{\partial y} + \frac{\partial w c_\ell}{\partial z} = \frac{\partial}{\partial x}\left(K_H \frac{\partial c_\ell}{\partial x}\right) + \frac{\partial}{\partial y}\left(K_H \frac{\partial c_\ell}{\partial y}\right)$$

$$+ \frac{\partial}{\partial z}\left(K_V \frac{\partial c_\ell}{\partial z}\right) + R_\ell(c_1, c_2, \ldots, c_p) + S_\ell \qquad (1)$$

$$\ell = 1, 2, \ldots, p$$

for

$$x_W \leq x \leq x_E$$

$$y_S \leq y \leq y_N$$

$$h(x,y) \leq z \leq H(x,y,t)$$

$$t \geq t_o$$

where

x,y = horizontal coordinates

z = vertical coordinate

u,v,w = the three deterministic components of the wind vector

c_ℓ = mean concentration of species ℓ

K_H, K_V = horizontal and vertical turbulent diffusivities

S_ℓ = rate of emission of species ℓ from elevated sources

R_ℓ = rate of production of species ℓ through chemical reaction

x_W, x_E, y_S, y_N = west, east, south, and north model boundaries

$h(x,y)$ = terrain elevation

$H(x,y,t)$ = inversion base elevation

Equation (1) must be solved subject to initial and boundary conditions. The initial condition is

$$c_\ell(x,y,z,t_o) = f_\ell(x,y,z) \tag{2}$$

where f_ℓ is the initial concentration distribution of species ℓ. The boundary conditions that apply at the ground and inversion base are:

(1) $z = h(x,y)$

$$-(\underline{\underline{K}} \cdot \underline{\nabla} c_\ell) \cdot \underline{n}_h = Q_\ell(x,y,t) \tag{3}$$

where

$$\underline{\underline{K}} = \begin{pmatrix} K_H & 0 & 0 \\ 0 & K_H & 0 \\ 0 & 0 & K_V \end{pmatrix}$$

$\underline{n}_h$ is the unit vector normal to the terrain directed into the atmosphere, and Q_ℓ is the mass flux of species ℓ at the surface.*

* We indicate vector and tensor quantities through the use of single and double underbars, respectively.

(2) $z = H(x,y,t)$

$$(\underline{V}c_\ell - \underline{\underline{K}}\cdot\underline{\nabla}\cdot c_\ell)\cdot\underline{n}_H = \underline{V}\, g_\ell(x,y,z,t)\cdot\underline{n}_H \qquad \text{if } \underline{V}\cdot\underline{n}_H \leq 0$$

$$-(\underline{\underline{K}}\cdot\underline{\nabla}c_\ell)\cdot\underline{n}_H = 0 \qquad \text{if } \underline{V}\cdot\underline{n}_H > 0 \tag{4}$$

where $\underline{V}$ is the advective velocity of pollutants relative to the moving inversion base,

$$\underline{V} = u\underline{i} + v\underline{j} + (w - \frac{\partial H}{\partial t})\,\underline{k}$$

$\underline{n}_H$ is the unit vector normal to the surface defined by the inversion base and directed out of the modeling region, and g_ℓ is the mean concentration of species ℓ aloft (just above the inversion base).

The conditions that apply along the horizontal boundaries are:

(3) $x = x_W$ or x_E

$$(uc_\ell - K_H\frac{\partial c_\ell}{\partial x}) = ug_\ell \qquad \text{if } \underline{U}\cdot\underline{n} \leq 0$$

$$-K_H\frac{\partial c_\ell}{\partial x} = 0 \qquad \text{if } \underline{U}\cdot\underline{n} > 0 \tag{5}$$

(4) $y = y_S$ or y_N

$$(vc_\ell - K_H\frac{\partial c_\ell}{\partial y}) = vg_\ell \qquad \text{if } \underline{U}\cdot\underline{n} \leq 0$$

$$-K_H\frac{\partial c_\ell}{\partial y} = 0 \qquad \text{if } \underline{U}\cdot\underline{n} > 0 \tag{6}$$

where $\underline{U} = u\underline{i} + v\underline{j}$, $\underline{n}$ is the outwardly directed unit vector normal to the horizontal boundary, and g_ℓ is the mean concentration of species ℓ just outside the airshed boundary.

These equations, which are a repetition of Equations (5) - (9) in the Final Report, are coupled since they share a common argument in the chemical reaction terms $R_\ell(c_1, c_2, \ldots, c_p)$. In the present version of the model, we simulate the dynamic behavior of six chemical species --reactive and unreactive hydrocarbon, NO, NO_2, O_3, and CO. The extent to which "unreactive" hydrocarbon and CO participate in chemical reactions is generally small, and hence we have set R_ℓ equal to zero in Equation (1) for these two species. Consequently, we must solve a system of four coupled, nonlinear partial differential equations involving reactive hydrocarbon, NO, NO_2, and O_3, and two sets of linear partial differential equations involving unreactive hydrocarbon and CO.

In Appendix D of Roth et al. (1971), we formulated a numerical scheme based on the method of fractional steps for the solution of equations similar to (1) - (6), the only difference being that horizontal diffusion was ignored. The method of fractional steps, discussed by Yanenko (1971), was especially developed to treat multidimensional problems arising in mathematical physics. The characteristic feature of the method is that the solution of a multidimensional problem is replaced by the successive solution of several problems having fewer dimensions. For example, a four-dimensional equation in (x,y,z,t) space may be split into three two-dimensional equations, in (x,t), (y,t), and (z,t) space.

One of the primary considerations regarding the use of finite-difference methods for the solution of Equation (1) is the manner in which the advection terms are to be approximated. In Appendix D of Roth et al. (1971), we discussed this problem and proposed to study two high-order techniques--a second-order scheme given by Crowley (1968), and a fourth-order scheme devised by Fromm (1969). After further examination of these two schemes, we found that both had the unfortunate property of producing negative concentrations in areas on the grid where large concentration gradients occurred. Thus, to avoid negative concentrations and yet maintain the accuracy of a high-order technique, we implemented another second-order scheme, described by Price et al. (1966), which we found to be capable of handling gradients without producing negative concentrations. We discuss the application of this method in more detail in Section III.

In the next section we describe the algorithms used to obtain the numerical solution of Equations (1) - (6). First, we perform a change of

variables that transforms the region between the ground and the inversion base from an irregular to a rectangular region. In so doing, we write the transformed equations in a way that makes it possible to use a *conservative* finite-difference representation. Second, we formulate all finite-difference schemes in a conservative manner. And finally, we employ a Newton iterative procedure to solve the nonlinear equations which result from the implicit finite-difference treatment of the (z,t) fragment.

In Section II, we include the recursive formulas used to solve the systems of linear equations which result from the application of the implicit finite-difference methods described in Section I.

The last section of this Appendix is devoted to a discussion of the numerical method. We explain the difficulties encountered in the application of advective difference approximations, and the manner in which they were overcome. To evaluate the numerical treatment of the nonlinear chemical reaction terms, we have conducted two tests of the numerical method. The results of these tests are presented and discussed in Section III.

I. THE METHOD OF FRACTIONAL STEPS APPLIED TO THE INTEGRATION OF THE MASS CONSERVATION EQUATIONS

In this section we discuss in detail the numerical solution of Equations (1), six partial differential equations in three spatial dimensions and time. The problem is complicated by the fact that four of the equations are coupled and nonlinear due to the appearance of the chemical reaction term R_ℓ. To apply the method of fractional steps, we fragment the original four-dimensional equation (x,y,z,t) into three two-dimensional partial differential equations in (x,t), (y,t), and (z,t) respectively. We include the chemical reaction and elevated source terms, R_ℓ and S_ℓ, in the (z,t) fragment. The solution of the (x,t) and (y,t) fragments is explicit, while the solution of the (z,t) fragment is implicit. To compute an integration time step, we successively solve the equations representative of the (x,t), (y,t), and (z,t) fragments. Before presenting the details of the finite-difference equations, however, we first discuss certain aspects of the equations and their solution.

A. Transformation of the Governing Equations

The modeling region, as defined, is bounded in the vertical by the ground and the base of the elevated inversion. We designate the elevation difference between these two boundaries as the mixing depth. One of the characteristic features of the mixing depth is that it varies with location (i.e., with x and y at a given time t). This variation is due in part to variations in terrain elevation, and in part to the general increase in the elevation of the inversion base with distance from the coast. We also note that the upper boundary changes position with time as the inversion base moves up, then down, during the course of a day. To implement the finite-difference scheme on a "fixed" rectangular grid, we perform the following change of variables:

$$\tau = t \tag{7a}$$

$$\xi = x \tag{7b}$$

$$\eta = y \tag{7c}$$

$$\rho = \frac{z-h(x,y)}{H(x,y,t)-h(x,y)} \tag{7d}$$

Under this change of variables, Equation (1) becomes

$$\frac{\partial}{\partial\tau}\left(\Delta H c_\ell\right) + \frac{\partial}{\partial\xi}\left(u\Delta H c_\ell\right) + \frac{\partial}{\partial\eta}\left(v\Delta H c_\ell\right) + \frac{\partial}{\partial\rho}\left(W c_\ell\right)$$

$$= \frac{\partial}{\partial\xi}\left[K_H\Delta H\frac{\partial c_\ell}{\partial\xi} - K_H\left(\frac{\partial h}{\partial\xi} + \rho\frac{\partial\Delta H}{\partial\xi}\right)\frac{\partial c_\ell}{\partial\rho}\right]$$

$$+ \frac{\partial}{\partial\eta}\left[K_H\Delta H\frac{\partial c_\ell}{\partial\eta} - K_H\left(\frac{\partial h}{\partial\eta} + \rho\frac{\partial\Delta H}{\partial\eta}\right)\frac{\partial c_\ell}{\partial\rho}\right]$$

$$+ \frac{\partial}{\partial\rho}\left[-K_H\left(\frac{\partial h}{\partial\xi} + \rho\frac{\partial\Delta H}{\partial\xi}\right)\frac{\partial c_\ell}{\partial\xi} - K_H\left(\frac{\partial h}{\partial\eta} + \rho\frac{\partial\Delta H}{\partial\eta}\right)\frac{\partial c_\ell}{\partial\eta}\right.$$

$$\left. + \left(\frac{K_H}{\Delta H}\left(\frac{\partial h}{\partial\xi} + \rho\frac{\partial\Delta H}{\partial\xi}\right)^2 + \frac{K_H}{\Delta H}\left(\frac{\partial h}{\partial\eta} + \rho\frac{\partial\Delta H}{\partial\eta}\right)^2 + \frac{K_V}{\Delta H}\right)\frac{\partial c_\ell}{\partial\rho}\right]$$

$$+ R_\ell\Delta H + S_\ell\Delta H \qquad \ell = 1,2,\ldots,p \tag{8}$$

where

$$\begin{aligned} \Delta H &= H(\xi,\eta,\tau) - h(\xi,\eta) \\ W &= w - u\left(\frac{\partial h}{\partial\xi} + \rho\frac{\partial\Delta H}{\partial\xi}\right) - v\left(\frac{\partial h}{\partial\eta} + \rho\frac{\partial\Delta H}{\partial\eta}\right) - \rho\frac{\partial\Delta H}{\partial\tau} \end{aligned} \tag{9}$$

The initial and boundary conditions become:

$$c_\ell(\xi,\eta,\rho,\tau_o) = f_\ell(\xi,\eta,\rho) \tag{10}$$

(1) $\rho = 0$

$$Q_\ell(\xi,\eta,\tau) = -\left[\frac{K_H}{\Delta H}\left(\frac{\partial h}{\partial \xi}\right)^2 + \frac{K_H}{\Delta H}\left(\frac{\partial h}{\partial \eta}\right)^2 + \frac{K_V}{\Delta H}\right]\frac{\partial c_\ell}{\partial \rho}$$

$$+ K_H\left(\frac{\partial h}{\partial \xi}\right)\frac{\partial c_\ell}{\partial \xi} + K_H\left(\frac{\partial h}{\partial \eta}\right)\frac{\partial c_\ell}{\partial \eta} \qquad (11)$$

(2) $\rho = 1$

$$Wg_\ell = Wc_\ell + K_H\left(\frac{\partial H}{\partial \xi}\right)\frac{\partial c_\ell}{\partial \xi} + K_H\left(\frac{\partial H}{\partial \eta}\right)\frac{\partial c_\ell}{\partial \eta}$$

$$- \left(\frac{K_H}{\Delta H}\left(\frac{\partial H}{\partial \xi}\right)^2 + \frac{K_H}{\Delta H}\left(\frac{\partial H}{\partial \eta}\right)^2 + \frac{K_V}{\Delta H}\right)\frac{\partial c_\ell}{\partial \rho} \qquad \text{if } W \leq 0$$

$$0 = K_H\left(\frac{\partial H}{\partial \xi}\right)\frac{\partial c_\ell}{\partial \xi} + K_H\left(\frac{\partial H}{\partial \eta}\right)\frac{\partial c_\ell}{\partial \eta} - \left(\frac{K_H}{\Delta H}\left(\frac{\partial H}{\partial \xi}\right)^2 + \frac{K_H}{\Delta H}\left(\frac{\partial H}{\partial \eta}\right)^2\right.$$

$$\left. + \frac{K_V}{\Delta H}\right)\frac{\partial c_\ell}{\partial \rho} \qquad (12) \qquad \text{if } W > 0$$

(3) $\xi = \xi_E$ or ξ_W

$$uc_\ell - K_H\left(\frac{\partial c_\ell}{\partial \xi} - \frac{1}{\Delta H}\left(\frac{\partial h}{\partial \xi} + \rho\frac{\partial \Delta H}{\partial \xi}\right)\frac{\partial c_\ell}{\partial \rho}\right) = ug_\ell \qquad \text{if } \underline{U}\cdot\underline{n} \leq 0$$

$$- K_H\left(\frac{\partial c_\ell}{\partial \xi} - \frac{1}{\Delta H}\left(\frac{\partial h}{\partial \xi} + \rho\frac{\partial \Delta H}{\partial \xi}\right)\frac{\partial c_\ell}{\partial \rho}\right) = 0 \qquad \text{if } \underline{U}\cdot\underline{n} > 0 \qquad (13)$$

(4) $\eta = \eta_S$ or η_N

$$vc_\ell - K_H\left(\frac{\partial c_\ell}{\partial \eta} - \frac{1}{\Delta H}\left(\frac{\partial h}{\partial \eta} + \rho\frac{\partial \Delta H}{\partial \eta}\right)\frac{\partial c_\ell}{\partial \rho}\right) = vg_\ell \qquad \text{if } \underline{U}\cdot\underline{n} \leq 0$$

$$- K_H\left(\frac{\partial c_\ell}{\partial \eta} - \frac{1}{\Delta H}\left(\frac{\partial h}{\partial \eta} + \rho\frac{\partial \Delta H}{\partial \eta}\right)\frac{\partial c_\ell}{\partial \rho}\right) = 0 \qquad \text{if } \underline{U}\cdot\underline{n} > 0 \tag{14}$$

In the application of Equations (8) - (14) to the computation of pollutant concentrations in the Los Angeles Basin, several terms in the above equations are generally small with respect to other terms and therefore can be neglected. Changes in the terrain and inversion base elevation with location are gradual, indicating that the derivatives $\partial h/\partial \xi$, $\partial h/\partial \eta$, $\partial \Delta H/\partial \xi$ and $\partial \Delta H/\partial \eta$ are considerably smaller than one. With the assumption that terms in Equation (8) containing these derivatives can be neglected,* Equation (8) becomes

$$\frac{\partial}{\partial \tau}(\Delta H c_\ell) + \frac{\partial}{\partial \xi}(u\Delta H c_\ell) + \frac{\partial}{\partial \eta}(v\Delta H c_\ell) + \frac{\partial}{\partial \rho}(W c_\ell)$$

$$= \frac{\partial}{\partial \xi}\left(K_H \Delta H \frac{\partial c_\ell}{\partial \xi}\right) + \frac{\partial}{\partial \eta}\left(K_H \Delta H \frac{\partial c_\ell}{\partial \eta}\right) + \frac{\partial}{\partial \rho}\left(\frac{K_V}{\Delta H}\frac{\partial c_\ell}{\partial \rho}\right)$$

$$+ R_\ell \Delta H + S_\ell \Delta H \qquad \ell = 1,2,\ldots,p \tag{15}$$

We note that, whereas the assumption is valid that the derivatives $\partial h/\partial \xi$, $\partial h/\partial \eta$, $\partial \Delta H/\partial \xi$ and $\partial \Delta H/\partial \eta$ are small in the flat portions of the Los Angeles airshed, it does not hold in the mountainous areas, such as the Palos Verdes Hills and the Santa Monica Mountains. However, since the terms omitted in Equation (15) involve horizontal diffusion, which is generally less important than horizontal advection, we do not expect to incur exceptionally large errors in using Equation (15). In the application to a

* To properly account for convergence and divergence effects, W is still given by Equation (9). See Equations (71) - (76) for a description of the evaluation of W .

different airshed in which topographical effects are of prime importance, it would be desirable to use Equations (8) - (14) as the basis of the model.

Under the assumptions invoked in obtaining Equation (15), the initial and boundary conditions become:

$$c_\ell(\xi,\eta,\rho,\tau_o) = f_\ell(\xi,\eta,\rho) \tag{16}$$

(1) $\rho = 0$

$$Q_\ell(\xi,\eta,\tau) = -\frac{K_V}{\Delta H}\frac{\partial c_\ell}{\partial \rho} \tag{17}$$

(2) $\rho = 1$

$$\begin{aligned} Wc_\ell - \frac{K_V}{\Delta H}\frac{\partial c_\ell}{\partial \rho} &= Wg_\ell && \text{if } W \leq 0 \\ -\frac{K_V}{\Delta H}\frac{\partial c_\ell}{\partial \rho} &= 0 && \text{if } W > 0 \end{aligned} \tag{18}$$

(3) $\xi = \xi_W$ or ξ_E

$$\begin{aligned} uc_\ell - K_H\frac{\partial c_\ell}{\partial \xi} &= ug_\ell && \text{if } \underline{U}\cdot\underline{n} \leq 0 \\ -K_H\frac{\partial c_\ell}{\partial \xi} &= 0 && \text{if } \underline{U}\cdot\underline{n} > 0 \end{aligned} \tag{19}$$

(4) $\eta = \eta_S$ or η_N

$$vc_\ell - K_H \frac{\partial c_\ell}{\partial \eta} = vg_\ell \qquad \text{if } \underline{U}\cdot\underline{n} \leq 0$$

$$- K_H \frac{\partial c_\ell}{\partial \eta} = 0 \qquad \text{if } \underline{U}\cdot\underline{n} > 0 \tag{20}$$

Thus we shall use Equations (15) - (20) as the basis for the simulation model of photochemical air pollution in the Los Angeles airshed. We note that these equations can be solved on a fixed rectangular grid with spacing $\Delta\xi$, $\Delta\eta$, and $\Delta\rho$.

B. The Computational Grid

Originally, a 25 x 25 x 5 grid network was adopted for the Los Angeles simulation study, where $\Delta\xi = \Delta\eta = 2$ miles, and $\Delta\rho = 0.2$ (ξ and η can be scaled by the length of the airshed, but this only introduces additional arithmatic operations into the finite-difference equations). Upon examining the 25 x 25 horizontal grid layout, we found that 198 of the 625 grid squares were over the Pacific Ocean and the San Gabriel Mountains--two areas having no emissions sources. Consequently, we eliminated these grid squares from the original grid to form the region over which the actual computations were performed. This amounted to a savings of approximately 30% in the required computing time. The grid is illustrated in Figure 1. Thus the computational grid consists of 2135 grid cells (427 horizontal grid squares x 5 vertical levels).

C. Nomenclature

The exposition of finite-difference schemes generally requires the use of subscripts and superscripts to denote spatial and temporal aspects of a particular variable. This application is no exception, and, in fact, is somewhat more complicated than most. We shall denote the concentration distribution on the grid by:

$${}^{m}_{\ell}c^{n}_{i,j,k}$$

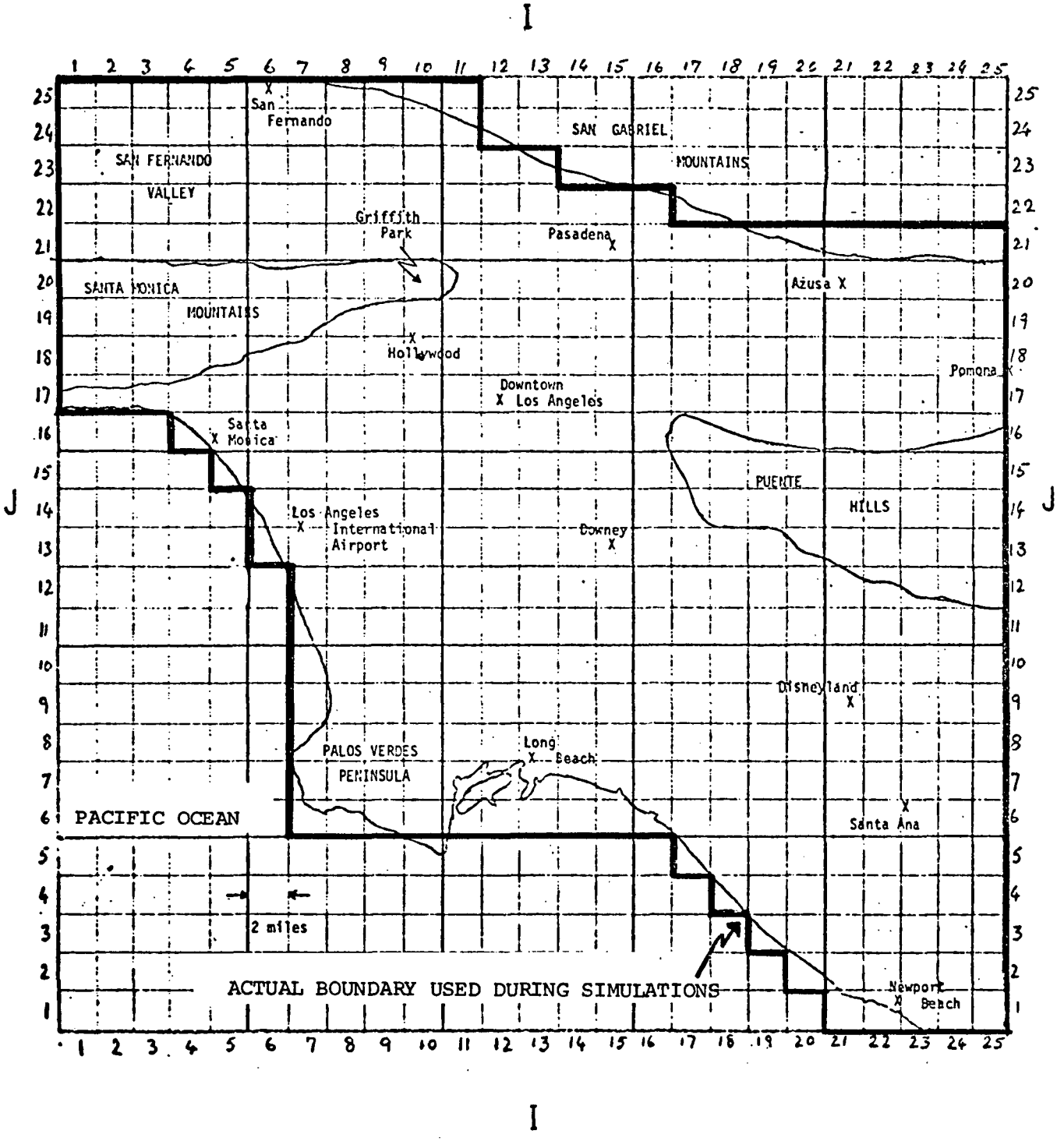

Figure 1. The Modeling Region

where ℓ is an index denoting chemical species, $1 \leq \ell \leq 6$

i,j,k are indices designating the grid cell location in the ξ-η-ρ coordinate system

$$I_W \leq i \leq I_E$$
$$J_S \leq j \leq J_N$$
$$1 \leq k \leq K$$

where I_W, I_E, J_S, and J_N indicate the column or row number of cells adjacent to the west, east, south, or north borders, and K is the number of vertical levels.

n is an index in time, $n \geq 0$

m refers to the iteration number, $m \geq 0$

We show subscripts and superscripts on other variables in an analogous manner.

D. Finite-Difference Equations

The method of fractional steps is applied to the solution of Equations (15) - (20) as follows. First, Equation (15) is split into three two-dimensional equations in (ξ,τ), (η,τ) and (ρ,τ). The three equations are given by:

Step I: $$\frac{\partial}{\partial\tau}(\Delta H c_\ell) + \frac{\partial}{\partial\xi}(u\Delta H c_\ell) = \frac{\partial}{\partial\xi}\left(K_H \Delta H \frac{\partial c_\ell}{\partial\xi}\right) \tag{21}$$

Step II: $$\frac{\partial}{\partial\tau}(\Delta H c_\ell) + \frac{\partial}{\partial\eta}(v\Delta H c_\ell) = \frac{\partial}{\partial\eta}\left(K_H \Delta H \frac{\partial c_\ell}{\partial\eta}\right) \tag{22}$$

Step III: $$\frac{\partial}{\partial\tau}(\Delta H c_\ell) + \frac{\partial}{\partial\rho}(W c_\ell) = \frac{\partial}{\partial\rho}\left(\frac{K_V}{\Delta H}\frac{\partial c_\ell}{\partial\rho}\right) + R_\ell \Delta H + S_\ell \Delta H \tag{23}$$

The calculation of ${}_\ell C^{n+1}_{i,j,k}$ given values of ${}_\ell C^{n}_{i,j,k}$ requires three steps:

Step I: Integration in the ξ direction
Step II: Integration in the η direction
Step III: Integration in the ρ direction

We now present the actual finite-difference expressions employed in the three-step integration procedure.

STEP I: Integration in the ξ Direction

We advance the concentration distribution at the nth time level, ${}_{\ell}C^{n}_{i,j,k}$, to the first intermediate time level, ${}_{\ell}C^{*}_{i,j,k}$, by integrating Equation (21) over the time interval $\Delta\tau$. The explicit, second-order finite difference expressions adopted for the spatial derivatives are based on the results of Price et al. (1966).

$$ {}_{\ell}C^{*}_{i,j,k} = {}_{\ell}C^{n}_{i,j,k} + \frac{\Delta\tau}{\Delta\xi\Delta H^{n}_{i,j}} \left({}_{\ell}F^{n}_{i-\frac{1}{2},j,k} - {}_{\ell}F^{n}_{i+\frac{1}{2},j,k} \right) \tag{24} $$

where

$$ \frac{\Delta\tau}{\Delta\xi} \; {}_{\ell}F^{n}_{i-\frac{1}{2},j,k} = \frac{\alpha^{n}_{i-\frac{1}{2},j,k}}{2} \left(3\,{}_{\ell}C^{n}_{i-1,j,k} - {}_{\ell}C^{n}_{i-2,j,k} \right) \tag{25} $$

$$ + \gamma^{n}_{i-\frac{1}{2},j,k} \left({}_{\ell}C^{n}_{i-1,j,k} - {}_{\ell}C^{n}_{i,j,k} \right) \quad \text{if } \alpha^{n}_{i-\frac{1}{2},j,k} \geq 0 $$

or

$$ \frac{\Delta\tau}{\Delta\xi} \; {}_{\ell}F^{n}_{i-\frac{1}{2},j,k} = \frac{\alpha^{n}_{i-\frac{1}{2},j,k}}{2} \left(3\,{}_{\ell}C^{n}_{i,j,k} - {}_{\ell}C^{n}_{i+1,j,k} \right) \tag{26} $$

$$ + \gamma^{n}_{i-\frac{1}{2},j,k} \left({}_{\ell}C^{n}_{i-1,j,k} - {}_{\ell}C^{n}_{i,j,k} \right) \quad \text{if } \alpha^{n}_{i-\frac{1}{2},j,k} < 0 $$

$$\alpha^n_{i-\frac{1}{2},j,k} = \frac{u^n_{i-\frac{1}{2},j,k}\ \Delta H^n_{i-\frac{1}{2},j}\ \Delta\tau}{\Delta\xi} \tag{27}$$

$$\gamma^n_{i-\frac{1}{2},j,k} = \frac{K^n_{H_{i-\frac{1}{2},j,k}}\ \Delta H^n_{i-\frac{1}{2},j}\ \Delta\tau}{\Delta\xi^2} \tag{28}$$

In Equation (24) we have made the following assumption with regard to the evaluation of ΔH at the first intermediate time level:

$$\Delta H^*_{i,j} = \Delta H^n_{i,j}$$

Since the effects of temporal mixing depth changes on pollutant concentrations are best treated in Step III, we defer movement of the inversion to that point in the computational scheme.

When applying Equation (24) in grid cells adjacent to the western or eastern borders (ξ_W or ξ_E), we employ the expressions for the boundary conditions given in Equation (19). Thus, grid cells adjacent to the western border (ξ_W) are treated as follows:

$$\ell C^*_{I_W,j,k} = \ell C^n_{I_W,j,k} + \frac{\Delta\tau}{\Delta\xi\Delta H^n_{I_W,j}}\left(\ell F^n_{I_W-\frac{1}{2},j,k} - \ell F^n_{I_W+\frac{1}{2},j,k}\right) \tag{29}$$

where

$$\frac{\Delta\tau}{\Delta\xi}\ \ell F^n_{I_W-\frac{1}{2},j,k} = \left(\alpha^n_{I_W-\frac{1}{2},j,k}\right)\ \ell g^n_{I_W-\frac{1}{2},j,k} \qquad \text{if } \alpha^n_{I_W-\frac{1}{2},j,k} \geq 0 \tag{30}$$

$$\frac{\Delta\tau}{\Delta\xi}\ \ell F^n_{I_W-\frac{1}{2},j,k} = \frac{\alpha^n_{I_W-\frac{1}{2},j,k}}{2}\left(3\ell C^n_{I_W,j,k} - \ell C^n_{I_W+1,j,k}\right) \tag{31}$$

$$\text{if } \alpha^n_{I_W-\frac{1}{2},j,k} < 0$$

and

$$\frac{\Delta\tau}{\Delta\xi}\ {}_{\ell}F^{n}_{I_w+\frac{1}{2},j,k} = \frac{\alpha^{n}_{I_w+\frac{1}{2},j,k}}{2}\left(3\,{}_{\ell}C^{n}_{I_w,j,k} - {}_{\ell}g^{n}_{I_w-\frac{1}{2},j,k}\right) \tag{32}$$

$$+\ \gamma^{n}_{I_w+\frac{1}{2},j,k}\left({}_{\ell}C^{n}_{I_w,j,k} - {}_{\ell}C^{n}_{I_w+1,j,k}\right)$$

$$\text{if } \alpha^{n}_{I_w+\frac{1}{2},j,k} \geq 0$$

$$\frac{\Delta\tau}{\Delta\xi}\ {}_{\ell}F^{n}_{I_w+\frac{1}{2},j,k} = \frac{\alpha^{n}_{I_w+\frac{1}{2},j,k}}{2}\left(3\,{}_{\ell}C^{n}_{I_w+1,j,k} - {}_{\ell}C^{n}_{I_w+2,j,k}\right) \tag{33}$$

$$+\ \gamma^{n}_{I_w+\frac{1}{2},j,k}\left({}_{\ell}C^{n}_{I_w,j,k} - {}_{\ell}C^{n}_{I_w+1,j,k}\right)$$

$$\text{if } \alpha_{I_w+\frac{1}{2},j,k} < 0$$

In Equation (32) we have replaced ${}_{\ell}C^{n}_{I_w-1,j,k}$ by ${}_{\ell}g^{n}_{I_w-\frac{1}{2},j,k}$ the value of the concentration outside the modeling region. The treatment at the eastern border (ξ_E) is analogous to that given for the western border above. It should be noted that in moving from grid cell to grid cell in the ξ direction, we need only compute

$$\frac{\Delta\tau}{\Delta\xi}\ {}_{\ell}F^{n}_{i+\frac{1}{2},j,k}$$

for grid cell (i,j,k), since

$$\frac{\Delta\tau}{\Delta\xi}\ {}_{\ell}F^{n}_{i-\frac{1}{2},j,k}$$

is available from the calculations performed in grid cell (i-1,j,k).

STEP II: Integration in the η *Direction*

In this step, we advance from the first level intermediate concentrations ${}_{\ell}C^{*}_{i,j,k}$ to the second level intermediate concentrations ${}_{\ell}C^{**}_{i,j,k}$ by the finite-difference analog of Equation (22). These equations are the η direction counterparts of Equations (24) - (33).

$$ {}_{\ell}C^{**}_{i,j,k} = {}_{\ell}C^{*}_{i,j,k} + \frac{\Delta\tau}{\Delta\eta\Delta H^{n}_{i,j}}\left({}_{\ell}F^{*}_{i,j-\frac{1}{2},k} - {}_{\ell}F^{*}_{i,j+\frac{1}{2},k}\right) \tag{34}$$

where

$$\frac{\Delta\tau}{\Delta\eta}\ {}_{\ell}F^{*}_{i,j-\frac{1}{2},k} = \frac{\beta^{n}_{i,j-\frac{1}{2},k}}{2}\left(3\,{}_{\ell}C^{*}_{i,j-1,k} - {}_{\ell}C^{*}_{i,j-2,k}\right)$$

$$+ \delta^{n}_{i,j-\frac{1}{2},k}\left({}_{\ell}C^{*}_{i,j-1,k} - {}_{\ell}C^{*}_{i,j,k}\right) \tag{35}$$

$$\text{if } \beta^{n}_{i,j-\frac{1}{2},k} \geq 0$$

$$\frac{\Delta\tau}{\Delta\eta}\,{}_{\ell}F^{*}_{i,j-\frac{1}{2},k} = \frac{\beta^{n}_{i,j-\frac{1}{2},k}}{2}\left(3\,{}_{\ell}C^{*}_{i,j,k} - {}_{\ell}C^{*}_{i,j+1,k}\right)$$

$$+ \delta^{n}_{i,j-\frac{1}{2},k}\left({}_{\ell}C^{*}_{i,j-1,k} - {}_{\ell}C^{*}_{i,j,k}\right) \tag{36}$$

$$\text{if } \beta^{n}_{i,j-\frac{1}{2},k} < 0$$

and

$$\beta^{n}_{i,j-\frac{1}{2},k} = \frac{v^{n}_{i,j-\frac{1}{2},k}\,\Delta H^{n}_{i,j-\frac{1}{2}}\,\Delta\tau}{\Delta\eta} \tag{37}$$

$$\delta^{n}_{i,j-\frac{1}{2},k} = \frac{K^{n}_{H_{i,j-\frac{1}{2},k}}\,\Delta H^{n}_{i,j-\frac{1}{2}}\,\Delta\tau}{\Delta\eta^{2}} \tag{38}$$

Using the expressions for the boundary conditions as given in Equation (20), grid cells adjacent to the southern border (η_S) are treated as follows:

$${}_{\ell}C^{**}_{i,J_s,k} = {}_{\ell}C^{*}_{i,J_s,k} + \frac{\Delta\tau}{\Delta\eta\,\Delta H^{n}_{i,J_s}}\left({}_{\ell}F^{*}_{i,J_s-\frac{1}{2},k} - {}_{\ell}F^{*}_{i,J_s+\frac{1}{2},k}\right) \tag{39}$$

where

$$\frac{\Delta\tau}{\Delta\eta}\,{}_{\ell}F^{*}_{i,J_s-\frac{1}{2},k} = \left(\beta^{n}_{i,J_s-\frac{1}{2},k}\right){}_{\ell}g^{n}_{i,J_s-\frac{1}{2},k} \qquad \text{if } \beta^{n}_{i,J_s-\frac{1}{2},k} \geq 0 \tag{40}$$

$$\frac{\Delta\tau}{\Delta\eta}\,{}_{\ell}F^{*}_{i,J_s-\frac{1}{2},k} = \frac{\beta^{n}_{i,J_s-\frac{1}{2},k}}{2}\left(3\,{}_{\ell}C^{*}_{i,J_s,k} - {}_{\ell}C^{*}_{i,J_s+1,k}\right) \tag{41}$$

$$\text{if } \beta^{n}_{i,J_s-\frac{1}{2},k} < 0$$

$$\frac{\Delta\tau}{\Delta\eta}\,{}_{\ell}F^{*}_{i,J_s+\frac{1}{2},k} = \frac{\beta^{n}_{i,J_s+\frac{1}{2},k}}{2}\left(3\,{}_{\ell}C^{*}_{i,J_s,k} - {}_{\ell}g^{n}_{i,J_s-\frac{1}{2},k}\right)$$

$$+\ \delta^{n}_{i,J_s+\frac{1}{2},k}\left({}_{\ell}C^{*}_{i,J_s,k} - {}_{\ell}C^{*}_{i,J_s+1,k}\right) \tag{42}$$

$$\text{if } \beta^{n}_{i,J_s+\frac{1}{2},k} \geq 0$$

$$\frac{\Delta\tau}{\Delta\eta}\,{}_{\ell}F^{*}_{i,J_s+\frac{1}{2},k} = \frac{\beta^{n}_{i,J_s+\frac{1}{2},k}}{2}\left(3\,{}_{\ell}C^{*}_{i,J_s+1,k} - {}_{\ell}C^{*}_{i,J_s+2,k}\right)$$

$$+\ \delta^{n}_{i,J_s+\frac{1}{2},k}\left({}_{\ell}C^{*}_{i,J_s,k} - {}_{\ell}C^{*}_{i,J_s+1,k}\right) \tag{43}$$

$$\text{if } \beta^{n}_{i,J_s+\frac{1}{2},k} < 0$$

The treatment of grid cells adjacent to the northern border (η_N) is analogous to that given for the southern border above.

STEP III: Integration in the ρ Direction

Having established values of ${}_{\ell}C^{**}_{i,j,k}$ from Step II, we now complete the integration procedure by solving a finite-difference approximation of Equation (23). These equations have been formulated in an implicit (Crank-Nicolson) manner to avert stability problems that might arise in the treatment of the diffusion term when the grid spacing is small due to a shallow mixing depth. In addition, the implicit formulation is also more suitable for treating the nonlinear chemical reaction terms.

$$
\begin{aligned}
{}_{\ell}C^{n+1}_{i,j,k} = {}_{\ell}C^{**}_{i,j,k} \frac{\Delta H^{n}_{i,j}}{\Delta H^{n+1}_{i,j}} &+ \frac{\Delta\tau}{2\Delta\rho\Delta H^{n+1}_{i,j}} \left({}_{\ell}F^{n+1}_{i,j,k-\frac{1}{2}} + {}_{\ell}F^{**}_{i,j,k-\frac{1}{2}} \right. \\
&\left. - {}_{\ell}F^{n+1}_{i,j,k+\frac{1}{2}} - {}_{\ell}F^{**}_{i,j,k+\frac{1}{2}} \right) + \frac{\Delta\tau}{2\Delta H^{n+1}_{i,j}} \left({}_{\ell}R^{n+1}_{i,j,k} \Delta H^{n+1}_{i,j} \right. \\
&\left. + {}_{\ell}R^{**}_{i,j,k} \Delta H^{n}_{i,j} \right) + \frac{\Delta\tau}{2\Delta H^{n+1}_{i,j}} \left({}_{\ell}S^{n+1}_{i,j,k} \Delta H^{n+1}_{i,j} + {}_{\ell}S^{n}_{i,j,k} \Delta H^{n}_{i,j} \right)
\end{aligned}
\tag{44}
$$

where

$$
\begin{aligned}
\frac{\Delta\tau}{\Delta\rho} {}_{\ell}F^{n+1}_{i,j,k-\frac{1}{2}} &= \frac{\phi^{n+1}_{i,j,k-\frac{1}{2}}}{2} \left({}_{\ell}C^{n+1}_{i,j,k-1} + {}_{\ell}C^{n+1}_{i,j,k} \right) \\
&+ \mu^{n+1}_{i,j,k-\frac{1}{2}} \left({}_{\ell}C^{n+1}_{i,j,k-1} - {}_{\ell}C^{n+1}_{i,j,k} \right) \qquad k = 2,3,\ldots,K
\end{aligned}
\tag{45}
$$

$$
\begin{aligned}
\frac{\Delta\tau}{\Delta\rho} {}_{\ell}F^{**}_{i,j,k-\frac{1}{2}} &= \frac{\phi^{n}_{i,j,k-\frac{1}{2}}}{2} \left({}_{\ell}C^{**}_{i,j,k-1} + {}_{\ell}C^{**}_{i,j,k} \right) \\
&+ \mu^{n}_{i,j,k-\frac{1}{2}} \left({}_{\ell}C^{**}_{i,j,k-1} - {}_{\ell}C^{**}_{i,j,k} \right) \qquad k = 2,3,\ldots,K
\end{aligned}
\tag{46}
$$

$$\phi^{n}_{i,j,k-\frac{1}{2}} = \frac{W^{n}_{i,j,k-\frac{1}{2}} \Delta\tau}{\Delta\rho} \tag{47}$$

$$\mu^{n}_{i,j,k-\frac{1}{2}} = \frac{K^{n}_{V_{i,j,k-\frac{1}{2}}} \Delta\tau}{\Delta H^{n}_{i,j} \Delta\rho^{2}} \tag{48}$$

The boundary conditions at the ground are:

(1) $\rho = 0$

$$\frac{\Delta\tau}{\Delta\rho} \ell F^{n+1}_{i,j,\frac{1}{2}} = \frac{\Delta\tau}{\Delta\rho} \ell Q^{n+1}_{i,j} \tag{49}$$

$$\frac{\Delta\tau}{\Delta\rho} \ell F^{**}_{i,j,\frac{1}{2}} = \frac{\Delta\tau}{\Delta\rho} \ell Q^{n}_{i,j} \tag{50}$$

where $k = \frac{1}{2}$ is equivalent to $\rho = 0$

(2) $\rho = 1$

$$\frac{\Delta\tau}{\Delta\rho} F^{n+1}_{i,j,K+\frac{1}{2}} = \phi^{n+1}_{i,j,K+\frac{1}{2}} \ell g^{n+1}_{i,j,K+\frac{1}{2}} \qquad \text{if } \phi^{n+1}_{i,j,K+\frac{1}{2}} \leq 0 \tag{51}$$

$$\frac{\Delta\tau}{\Delta\rho} \ell F^{n+1}_{i,j,K+\frac{1}{2}} = \phi^{n+1}_{i,j,K+\frac{1}{2}} \ell C^{n+1}_{i,j,K} \qquad \text{if } \phi^{n+1}_{i,j,K+\frac{1}{2}} > 0 \tag{52}$$

$$\frac{\Delta\tau}{\Delta\rho}\ {}_{\ell}F^{**}_{i,j,K+\frac{1}{2}} = \phi^{n}_{i,j,K+\frac{1}{2}}\ {}_{\ell}g^{n}_{i,j,K+\frac{1}{2}} \qquad \text{if } \phi^{n}_{i,j,K+\frac{1}{2}} \leq 0 \tag{53}$$

$$\frac{\Delta\tau}{\Delta\rho}\ {}_{\ell}F^{**}_{i,j,K+\frac{1}{2}} = \phi^{n}_{i,j,K+\frac{1}{2}}\ {}_{\ell}C^{**}_{i,j,K} \qquad \text{if } \phi^{n}_{i,j,K+\frac{1}{2}} > 0 \tag{54}$$

where $k = K+\frac{1}{2}$ is equivalent to $\rho = 1$.

At this point we need to discuss the following three topics:

1) Step III applied to inert species
2) Step III applied to chemically reactive species
3) The calculation of W.

The Treatment of Inert Species

For those species which are treated as being chemically inert, we set ${}_{\ell}R^{n}_{i,j,k} = 0$. The difference equations for Step III reduce to a system of linear equations involving the values of ${}_{\ell}C^{n+1}_{i,j,k}$. We can write the linear system for species ℓ as follows:

$$
\begin{bmatrix}
b_1 & c_1 & & & \\
a_2 & b_2 & c_2 & & \\
 & \ddots & \ddots & \ddots & \\
 & & a_{K-1} & b_{K-1} & c_{K-1} \\
 & & & a_K & b_K
\end{bmatrix}
\begin{bmatrix}
{}_{\ell}C^{n+1}_{i,j,1} \\
{}_{\ell}C^{n+1}_{i,j,2} \\
\vdots \\
{}_{\ell}C^{n+1}_{i,j,K-1} \\
{}_{\ell}C^{n+1}_{i,j,K}
\end{bmatrix}
=
\begin{bmatrix}
y_1 \\
y_2 \\
\vdots \\
y_{K-1} \\
y_K
\end{bmatrix}
\qquad (55)
$$

where the elements of the matrix and the column vector on the right-hand side of the equation can easily be determined using the finite-difference expressions given in Step III. We describe the algorithm used to solve this tridiagonal system of linear equations in Section II.

The Treatment of Chemically Reactive Species

The computation of vertical transport coupled with chemical reaction is the most complicated step in the numerical procedure. We will thus discuss this aspect of Step III in more detail. We recall that reactive hydrocarbon (HC), NO, NO_2, and O_3 are all coupled through the chemical reaction terms. Therefore, we are confronted with solving a system of nonlinear algebraic equations in 4K unknowns, where K is the number of vertical levels. In the present simulation effort, we employ five vertical levels, and so we must solve twenty nonlinear equations in twenty unknowns, where the unknowns are the values of ${}_{\ell}C^{n+1}_{i,j,k}$, $1 \leq k \leq 5$, for HC,NO,NO_2, and O_3.

To solve the system of nonlinear equations, we use a Newton iterative procedure. We begin by introducing the iterates ${}^{m}_{\ell}C^{n+1}_{i,j,k}$. Using Equation (23), the initial values of the iterates, ${}^{o}_{\ell}C^{n+1}_{i,j,k}$, are given by the following slightly modified Taylor series expansion

$$
\begin{aligned}
{}^{o}_{\ell}C^{n+1}_{i,j,k} = {}_{\ell}C^{**}_{i,j,k} \frac{\Delta H^{n}_{i,j}}{\Delta H^{n+1}_{i,j}} + \frac{\Delta\tau}{\Delta\rho\, \Delta H^{n+1}_{i,j}} \left({}_{\ell}F^{**}_{i,j,k-\frac{1}{2}} - {}_{\ell}F^{**}_{i,j,k+\frac{1}{2}} \right) \\
+ \frac{\Delta\tau}{\Delta H^{n+1}_{i,j}} \left({}_{\ell}R^{**}_{i,j,k}\, \Delta H^{n}_{i,j} \right) + \frac{\Delta\tau}{2\Delta H^{n+1}_{i,j}} \left({}_{\ell}S^{n+1}_{i,j,k}\, \Delta H^{n+1}_{i,j} \right. \\
\left. + {}_{\ell}S^{n}_{i,j,k}\, \Delta H^{n}_{i,j} \right)
\end{aligned}
\tag{56}
$$

The difference expressions for the terms in Equation (56) are given in Equations (45) - (54). Higher iterates are obtained by setting

$$
{}^{m+1}_{\ell}C^{n+1}_{i,j,k} = {}^{m}_{\ell}C^{n+1}_{i,j,k} + {}^{m}_{\ell}\delta C^{n+1}_{i,j,k} \tag{57}
$$

Next, we substitute the right-hand side of Equation (57) into Equations (44) - (54) in place of ${}_{\ell}C^{n+1}_{i,j,k}$ and neglect all quadratic terms involving ${}^{m}_{\ell}\delta C^{n+1}_{i,j,k}$. We can write the resulting system of linear equations in the following form:

$$
\begin{bmatrix}
{}^{m}B_1 & E_1 & & & \\
A_2 & {}^{m}B_2 & E_2 & & \\
 & \ddots & \ddots & \ddots & \\
 & & A_{K-1} & {}^{m}B_{K-1} & E_{K-1} \\
 & & & A_K & {}^{m}B_K
\end{bmatrix}
\begin{bmatrix}
{}^{m}\delta X_1 \\ {}^{m}\delta X_2 \\ \vdots \\ {}^{m}\delta X_{K-1} \\ {}^{m}\delta X_K
\end{bmatrix}
=
\begin{bmatrix}
{}^{m}P_1 \\ {}^{m}P_2 \\ \vdots \\ {}^{m}P_{K-1} \\ {}^{m}P_K
\end{bmatrix}
\tag{58}
$$

where A_k, ${}^mB_k$ and E_k are 4 x 4 matrices, and ${}^m\delta X_k$ and ${}^mP_k$ are column vectors. The coefficient matrix is block-tridiagonal, and systems of equations in this form can be solved efficiently. The chemical reaction rate expressions are given in Appendix B of this report. We define below the elements of each matrix and column vector.

$$A_k = a_k \, I \qquad k = 2,3,\ldots,K \tag{59}$$

where

$$a_k = -\frac{1}{2\Delta H^{n+1}_{i,j}} \left(\frac{\phi^{n+1}_{i,j,k-\frac{1}{2}}}{2} + \mu^{n+1}_{i,j,k-\frac{1}{2}} \right) \tag{60}$$

and I is the 4 x 4 identity matrix

$$E_k = e_k \, I \qquad k = 1,2,\ldots,K-1 \tag{61}$$

where

$$e_k = \frac{1}{2\Delta H^{n+1}_{i,j}} \left(\frac{\phi^{n+1}_{i,j,k+\frac{1}{2}}}{2} - \mu^{n+1}_{i,j,k+\frac{1}{2}} \right) \tag{62}$$

$${}^mB_k = b_k \, I + \frac{\Delta\tau}{2} \, {}^mD_k \tag{63}$$

where

$$
b_k = \begin{cases}
1 + \dfrac{1}{2\Delta H^{n+1}_{i,j}} \left(\dfrac{\phi^{n+1}_{i,j,k+\frac{1}{2}}}{2} + \mu^{n+1}_{i,j,k+\frac{1}{2}} \right) & k = 1 \\[2ex]
1 + \dfrac{1}{2\Delta H^{n+1}_{i,j}} \left(\dfrac{\phi^{n+1}_{i,j,k+\frac{1}{2}} - \phi^{n+1}_{i,j,k-\frac{1}{2}}}{2} + \mu^{n+1}_{i,j,k-\frac{1}{2}} + \mu^{n+1}_{i,j,k+\frac{1}{2}} \right) & k = 2,3,\ldots,K-1 \\[2ex]
1 + \dfrac{1}{2\Delta H^{n+1}_{i,j}} \left(\dfrac{2\phi^{n+1}_{i,j,K+\frac{1}{2}} - \phi^{n+1}_{i,j,K-\frac{1}{2}}}{2} + \mu^{n+1}_{i,j,K-\frac{1}{2}} \right) & k = K, \; W^{n+1}_{i,j,K+\frac{1}{2}} > 0 \\[2ex]
1 + \dfrac{1}{2\Delta H^{n+1}_{i,j}} \left(- \dfrac{\phi^{n+1}_{i,j,K-\frac{1}{2}}}{2} + \mu^{n+1}_{i,j,K-\frac{1}{2}} \right) & k = K, \; W^{n+1}_{i,j,K+\frac{1}{2}} \leq 0
\end{cases} \tag{64}
$$

$$
{}^{m}D_k = \begin{bmatrix} d_{11} & d_{12} & d_{13} & d_{14} \\ d_{21} & d_{22} & d_{23} & d_{24} \\ d_{31} & d_{32} & d_{33} & d_{34} \\ d_{41} & d_{42} & d_{43} & d_{44} \end{bmatrix} \tag{65}
$$

where

$$d_{11} = k_{11}O + k_{12}OH + k_{13}O_3$$

$$d_{12} = d_{21} = d_{14} = d_{41} = 0$$

$$d_{13} = k_{13}HC$$

$$d_{22} = k_3O_3 + k_6NO_2 + k_9HO_2 + k_{14}RO_2$$

$$d_{23} = k_3NO$$

$$d_{24} = k_6NO - k_1$$

$$d_{31} = k_{13}O_3$$

$$d_{32} = k_3O_3$$

$$d_{33} = k_3NO + k_4NO_2 + k_{13}HC$$

$$d_{34} = k_4O_3$$

$$d_{42} = k_6NO_2 - k_3O_3 - k_9HO_2 - k_{14}RO_2$$

$$d_{43} = k_4NO_2 - k_3NO$$

$$d_{44} = k_1 + k_4O_3 + k_5NO_3 + k_6NO + k_{10}HO_2 + k_{15}RO_2$$

and

$$HC = {}^{m}_{1}C^{n+1}_{i,j,k}$$

$$NO = {}^{m}_{2}C^{n+1}_{i,j,k}$$

$$O_3 = {}^{m}_{3}C^{n+1}_{i,j,k}$$

$$NO_2 = {}^{m}_{4}C^{n+1}_{i,j,k}$$

The expressions for the steady-state species O, OH, HO_2, RO_2, and NO_3 appearing in the matrices ${}^{m}D_k$ (see Equation (65)) are evaluated using the values of ${}^{m}_{\ell}C^{n+1}_{i,j,k}$. See Appendix B for the expressions relating the concentrations of the steady-state species to the concentrations of HC, NO, NO_2, and O_3. The remaining terms in Equation (58) are defined by:

$$ {}^{m}\delta X_k = \begin{bmatrix} {}^{m}_{1}\delta C^{n+1}_{i,j,k} \\ {}^{m}_{2}\delta C^{n+1}_{i,j,k} \\ {}^{m}_{3}\delta C^{n+1}_{i,j,k} \\ {}^{m}_{4}\delta C^{n+1}_{i,j,k} \end{bmatrix} \tag{66} $$

$$ {}^{m}P_k = P_k + {}^{m}\bar{P}_k \tag{67} $$

where

$$ P_k = \begin{bmatrix} {}_{1}P_k \\ {}_{2}P_k \\ {}_{3}P_k \\ {}_{4}P_k \end{bmatrix} \quad \text{and} \quad {}^{m}\bar{P}_k = \begin{bmatrix} {}^{m}\bar{}_{1}P_k \\ {}^{m}\bar{}_{2}P_k \\ {}^{m}\bar{}_{3}P_k \\ {}^{m}\bar{}_{4}P_k \end{bmatrix} \tag{68} $$

and

$$
{}_{\ell}P_k = {}_{\ell}C^{**}_{i,j,k} \frac{\Delta H^n_{i,j}}{\Delta H^{n+1}_{i,j}} + \frac{\Delta\tau}{2\Delta\rho\Delta H^{n+1}_{i,j}} \left({}_{\ell}F^{**}_{i,j,k-\frac{1}{2}} - {}_{\ell}F^{**}_{k,j,k+\frac{1}{2}} \right) \tag{69}
$$

$$
+ \frac{\Delta\tau}{2\Delta H^{n+1}_{i,j}} \left({}_{\ell}R^{**}_{i,j,k}\Delta H^n_{i,j} + {}_{\ell}S^{n+1}_{i,j,k}\Delta H^{n+1}_{i,j,} + {}_{\ell}S^{n}_{i,j,k}\Delta H^{n}_{i,j} \right)
$$

$$
{}^{m}_{\ell}\bar{P}_k = - {}^{m}_{\ell}C^{n+1}_{i,j,k} + \frac{\Delta\tau}{2\Delta\rho\Delta H^{n+1}_{i,j}} \left({}^{m}_{\ell}F^{n+1}_{i,j,k-\frac{1}{2}} - {}^{m}_{\ell}F^{n+1}_{i,j,k+\frac{1}{2}} \right)
$$

$$
+ \frac{\Delta\tau}{2\Delta H^{n+1}_{i,j}} \left({}^{m}_{\ell}R^{n+1}_{i,j,k}\Delta H^{n+1}_{i,j} \right) \tag{70}
$$

We note that each iteration involving the solution of Equation (58) requires only the additional evaluation of ${}^{m}D_k$ and ${}^{m}\bar{P}_k$ before the system can be solved, since all other terms are invariant from one iteration to the next. Thus we establish the matrices A_k, $b_k I$, and E_k, and the column vectors P_k. To perform an iteration, we evaluate ${}^{m}D_k$ and ${}^{m}\bar{P}_k$, and using Equations (63) and (67) we complete the definition of the linear system given by Equation (58). We describe the method used to solve this block-tridiagonal system of linear equations in Section II.

Upon solving Equation (58) for values of ${}^{m}_{\ell}\delta C^{n+1}_{i,j,k}$, we use Equation (57) to obtain an improved estimate of ${}^{\ell}C^{n+1}_{i,j,k}$. We terminate the iterative process when

$$\left| \frac{{}^{m}_{\ell}\delta C^{n+1}_{i,j,k}}{{}^{m}_{\ell}C^{n+1}_{i,j,k}} \right| \leq \varepsilon$$

for all ℓ and k in each column of grid cells. For the present simulation study, $\varepsilon = 0.01$.

The Evaluation of W

One of the assumptions commonly made in airshed modeling is that turbulent atmospheric flow is incompressible. Upon making this assumption, we can write:

$$\frac{\partial u}{\partial x} + \frac{\partial v}{\partial y} + \frac{\partial w}{\partial z} = 0 \tag{71}$$

or, in (ξ,η,ρ) coordinates

$$\frac{\partial u\Delta H}{\partial \xi} + \frac{\partial v\Delta H}{\partial \eta} + \frac{\partial \overline{W}}{\partial \rho} = 0 \tag{72}$$

where

$$\overline{W} = w - u\left(\frac{\partial h}{\partial \xi} + \rho\frac{\partial \Delta H}{\partial \xi}\right) - v\left(\frac{\partial h}{\partial \eta} + \rho\frac{\partial \Delta H}{\partial \eta}\right) \tag{73}$$

We note that W, as defined in Equation (9), is given by

$$W = \overline{W} - \rho\frac{\partial \Delta H}{\partial \tau} \tag{74}$$

Thus we use Equation (72) to solve for $\overline{W}$ and Equation (74) to evaluate W.

Equation (72) is integrated subject to the following boundary condition:

$$\overline{W} = 0 \qquad \text{at } \rho = 0 \tag{75}$$

This condition restricts the wind to flow parallel to the terrain at ground level. To obtain values of $\overline{W}$ from Equation (72), we write the following finite-difference equation:

$$\overline{W}^{n}_{i,j,k+\frac{1}{2}} = \overline{W}^{n}_{i,j,k-\frac{1}{2}} + \frac{\Delta\rho}{\Delta\xi}\left[(u\Delta H)^{n}_{i-\frac{1}{2},j,k} - (u\Delta H)^{n}_{i+\frac{1}{2},j,k}\right]$$

$$+ \frac{\Delta\rho}{\Delta\eta}\left[(v\Delta H)^{n}_{i,j-\frac{1}{2},k} - (v\Delta H)^{n}_{i,j+\frac{1}{2},k}\right] \tag{76}$$

$$\text{for } k = 1,2,\ldots,K$$

where

$$\overline{W}^{n}_{i,j,\frac{1}{2}} = 0$$

Note that Equation (76) requires knowledge of the vertical structure of the horizontal wind components. In the present simulation study, u and v are taken to be invariant with height.

This completes the presentation of Step III of the numerical integration procedure. We now turn our attention to discussing the stability characteristics of the difference equations. The basic statement that we can make with regard to stability is that if each step is stable, then the entire procedure is stable. Thus we examine each step individually to determine the conditions for stability, and we begin with Step I. To facilitate the analysis, we assume the u, ΔH and K_H are constants, and using the stability criteria given by Price et al. (1966), we obtain

$$\frac{u\Delta\tau}{\Delta\xi} + \frac{K_H\Delta\tau}{\Delta\xi^2} \leq \frac{1}{2}$$

We obtain a similar expression for Step II after making the analogous assumptions

$$\frac{v\Delta\tau}{\Delta\eta} + \frac{K_H\Delta\tau}{\Delta\eta^2} \leq \frac{1}{2}$$

Typically, the left-hand sides of these expressions are less than 0.3 for a grid spacing of two miles and a time step of four minutes.

Step III is more difficult to analyze since the equations are both coupled and nonlinear. We can, however, state the conditions for stability when the equations are linear, that is, when $R_\ell = 0$. Since we have employed the Crank-Nicolson treatment in this step, the solution is stable for all values of $\Delta\tau$. We must rely on numerical experimentation and experience to ascertain if the treatment of the full nonlinear set of equations is stable. We can report that, as of this writing, no evidence of instability has ever been observed.

II. METHODS FOR SOLVING THE LINEAR SYSTEMS OF EQUATIONS

In Step III of the numerical integration procedure, we must solve two systems of linear equations, each of the form

$$Ax = y$$

where the characteristics of the matrix A distinguish the first system from the second. The two forms assumed by matrix A are tridiagonal and block-triagonal, respectively. A tridiagonal matrix of order n can be written in the following manner:

$$\begin{bmatrix} A_{1,1} & A_{1,2} & & & & \\ A_{2,1} & A_{2,2} & A_{2,3} & & 0 & \\ & \ddots & \ddots & \ddots & & \\ & 0 & & A_{n-1,n-2} & A_{n-1,n-1} & A_{n-1,n} \\ & & & & A_{n,n-1} & A_{n,n} \end{bmatrix}$$

The block-tridiagonal matrix assumes the same form, but the distinguishing feature is that each element, $A_{i,j}$, is itself an $m \times m$ matrix. Thus the order of the matrix in this case is $n \cdot m$. We note that the tridiagonal matrix is actually a block-tridiagonal matrix with $m=1$. The algorithm employed to solve the block-tridiagonal system is equivalent to that used to solve the tridiagonal system, but we shall treat each separately for two reasons. First, the recursion formulas for the tridiagonal system are particularly simple to formulate; whereas, the recursion formulas for the block-tridiagonal system involve matrix inversions which need to be discussed in further detail. Second, we wish to formulate the algorithms using notation similar to that found in the computer codes described in Volume II.

A. The Algorithm for the Tridiagonal System

As the algorithm we have adopted for the solution of a tridiagonal system of linear equations is described in detail by Conte (1965), we only summarize the recursive formulas here. We wish to solve the following system of linear equations:

$$\begin{bmatrix} b_1 & c_1 & & & \\ a_2 & b_2 & c_2 & & \bigcirc \\ & \ddots & \ddots & \ddots & \\ \bigcirc & & a_{n-1} & b_{n-1} & c_{n-1} \\ & & & a_n & b_n \end{bmatrix} \begin{bmatrix} x_1 \\ x_2 \\ \vdots \\ x_{n-1} \\ x_n \end{bmatrix} = \begin{bmatrix} y_1 \\ y_2 \\ \vdots \\ y_{n-1} \\ y_n \end{bmatrix}$$

The solution vector x is obtained from the following four-step procedure:

(1) $\omega_1 = b_1$

$z_1 = y_1/\omega_1$

(2) Compute ω_i and z_i from

$\omega_i = b_i - a_i\, c_{i-1}/\omega_{i-1}$

$i = 2,3,\ldots,n-1$

$z_i = (y_i - a_i z_{i-1})/\omega_i$

(3) Set: $\omega_n = b_n - a_n c_{n-1}/\omega_{n-1}$

(4) Solve for the solution vector

$x_n = (y_n - a_n z_{n-1})/\omega_n$

$$x_{n-i} = z_{n-i} - c_{n-i}x_{n-i+1}/\omega_{n-i} \qquad i = 1,2,\ldots,n-1$$

This algorithm is the basis for the code in subroutine SIMDIG, which is part of the Atmospheric Pollution Simulation Program described in Volume II.

B. The Algorithm for the Block-Tridiagonal System

The algorithm described in this section is fashioned after that given by Isaacson and Keller (1966). Consider the following block-tridiagonal system of linear equations:

$$Ax = f \tag{77}$$

which we write as

$$\begin{bmatrix} B_1 & C_1 & & & & \\ A_2 & B_2 & C_2 & & \bigcirc & \\ & \ddots & \ddots & \ddots & & \\ & \bigcirc & & A_{n-1} & B_{n-1} & C_{n-1} \\ & & & & A_n & B_n \end{bmatrix} \begin{bmatrix} x_1 \\ x_2 \\ \vdots \\ x_{n-1} \\ x_n \end{bmatrix} = \begin{bmatrix} f_1 \\ f_2 \\ \vdots \\ f_{n-1} \\ f_n \end{bmatrix}$$

where A_i, B_i, and C_i are m x m matrices, and x_i and f_i are m-component column vectors. We write the coefficient matrix as the product of lower and upper triangular matrices in the following manner:

$$A = LU = \begin{bmatrix} D_1 & & & \\ A_2 & D_2 & & \bigcirc \\ & \ddots & \ddots & \\ \bigcirc & & A_n & D_n \end{bmatrix} \begin{bmatrix} I & \Gamma_1 & & \\ & \ddots & \ddots & \bigcirc \\ & & I & \Gamma_{n-1} \\ \bigcirc & & & I \end{bmatrix}$$

If we equate each element in A with each element in the matrix formed by the product LU, we can write the following identities

$$D_1 = B_1$$

$$\Gamma_1 = D_1^{-1} C_1 \tag{78}$$

$$D_i = B_i - A_i \Gamma_{i-1} \qquad i = 2,3,\ldots,n$$

$$\Gamma_i = D_i^{-1} C_i \qquad i = 2,3,\ldots,n-1 \tag{79}$$

Defining a new vector y, we note that Equation (77) is equivalent to

$$Ly = f \tag{80}$$

$$Ux = y \tag{81}$$

We proceed by solving Equation (80) for y, and then solving Equation (81) for x, which is the desired solution. The first step can be written as

$$y_1 = D_1^{-1} f_1 \tag{82}$$

$$y_i = D_i^{-1}(f_i - A_i y_{i-1}) \qquad i = 2,3,\ldots,n \tag{83}$$

and the second step is given by

$$x_n = y_n \tag{84}$$

$$x_{n-i} = y_{n-i} - \Gamma_{n-i} x_{n-i+1} \qquad i = 1,2,\ldots,n-1$$

The algorithm given above is formally correct, but we can improve upon it computationally in the following way. We write the following equivalent expressions for Equations (78) and (82), and Equations (79) and (83):

$$D_1\left(\Gamma_1 \vdots y_1\right) = \left(C_1 \vdots f_1\right) \tag{85}$$

$$D_i\left(\Gamma_i \vdots y_i\right) = \left(C_i \vdots f_i - A_i y_{i-1}\right) \qquad i = 2,3,\ldots,n \tag{86}$$

where the parentheses and dotted line indicate a partitioned matrix.*

We now summarize the algorithm in its final form.

(1) Set $D_1 = B_1$

(2) Solve for Γ_1 and y_1

$$D_1\left(\Gamma_1 \vdots y_1\right) = \left(C_1 \vdots f_1\right)$$

(3) Set

$$D_i = B_i - A_i \Gamma_{i-1}$$

$$i = 2,3,\ldots,n$$

$$\bar{f}_i = f_i - A_i y_{i-1}$$

* The partitioned matrix $(\Gamma_1 \vdots y_1)$ is formed by combining the m x m matrix Γ_1 with the m x 1 matrix y_1 to form a m x (m + 1) matrix.

(4) Solve for Γ_i and y_i

$$D_i \left(\Gamma_i \vdots y_i \right) = \left(C_i \vdots \bar{f}_i \right) \qquad i = 2,3,\ldots,n$$

(5) Set $$x_n = y_n$$

$$x_{n-i} = y_{n-i} - \Gamma_{n-i} x_{n-i+1} \qquad i = 1,2,\ldots,n-1$$

We solve the m+1 linear systems in steps (2) and (4) by Gaussian elimination. The five-step procedure given above serves as the basis for the code in subroutine BLCKTD, which is part of the Atmospheric Pollution Simulation Program described in Volume II.

III. DISCUSSION OF THE NUMERICAL METHOD

In Sections I and II, we have described the computational procedures employed in the solution of the governing airshed equations. In this section we recount our experiences in the formulation, testing, and application of the finite-difference expressions, as these experiences have had a direct bearing on our final choice of methods. We begin by discussing the horizontal advection-diffusion approximations which form the basis of Steps I and II. Of primary concern is the treatment of the advection terms, $\partial(uc)/\partial x$ and $\partial(vc)/\partial y$, since the effects of truncation error in the approximation of these terms may be important. Initially, we examined second and fourth-order schemes given by Crowley (1968) and Fromm (1969), respectively. After conducting tests involving the advection of hypothetical concentration distributions, we concluded that there was reasonable justification for adopting the more accurate fourth-order scheme.

Upon concluding these initial tests, we initiated an investigation to determine what effect the choice of method would have on the magnitudes of the predicted concentrations. Meteorological and source inputs used were typical of those employed in actual simulations. Unfortunately,

at the outset of this study, we observed that, during Steps I and II of the integration procedure, negative concentrations were predicted in the vicinity of coastal power plants by both the second and fourth-order finite-difference methods. When the vertical diffusion/chemical reaction calculations were carried out in these areas (i.e., Step III), the iterative procedure usually failed to converge. We concluded that the centered, high-order difference schemes may predict negative concentrations in areas on the grid where concentration gradients are large. One such area exists near coastal power plants since NO concentration levels in grid cells located over the ocean may differ substantially from those located just onshore.

We considered two alternatives that would eliminate this shortcoming in the numerical method. The first was to adopt another difference formulation of the advection terms which would not produce negative concentrations. A difference scheme that has this desirable characteristic is the simple first-order approximation. Although positive concentrations are predicted using this scheme, the method is not as accurate as the second and fourth-order methods. The second alternative was to specify a lower limit on the value of the predicted concentration in any grid cell. Thus, whenever a negative concentration is predicted, that concentration is set equal to some small value. Adoption of this alternative would have the effect of adding additional "sources" of pollutant to the model. During the time we were evaluating these two alternatives, we discovered the uncentered, second-order technique which we eventually adopted. The two important features that this scheme possesses are: 1) it is more accurate than the first-order scheme, and 2) it is capable of predicting positive concentrations in areas where relatively large concentration gradients exist. We performed advection tests using this uncentered second-order scheme and found that it was more accurate than the first-order scheme, but less accurate than the centered second-order scheme given by Crowley (1968). We finally adopted the uncentered second-order technique as a compromise between achieving accuracy on the one hand, and avoiding the possible calculation of negative concentrations on the other. Since the vertical concentration profiles are generally rather smooth and turbulent diffusion is the primary vertical transport mechanism, we have encountered no difficulties in approximating the advection and diffusion terms in Equation (23) with finite-difference expressions. The difference representation of $\partial(Wc_\ell)/\partial\sigma$, as given in Equation (45), is a centered, second-order approximation.

In addition to studying advection approximations for use in Steps I and II, we have also conducted a test of the finite-difference formulation used in Step III. The primary objective of this test is to evaluate the numerical treatment of the nonlinear chemical reaction terms. First we set all wind velocities and surface emissions fluxes equal to zero in a particular column of grid cells. We then established a uniform distribution of each pollutant in the column of cells and integrated the equations. The governing airshed equations reduce to the following form:

$$\frac{\partial c_\ell}{\partial t} = R_\ell \qquad \ell = 1,2,\ldots,p \tag{87}$$

which we recognize as the ordinary differential equations employed in simulating smog chamber experiments. We then solved Equations (87) using the method developed by Gear (1971) and compared the results. Using the following initial conditions:

$$\begin{aligned} HC &= 40 \text{ pphm} \\ NO &= 20 \text{ pphm} \\ O_3 &= 0.5 \text{ pphm} \\ NO_2 &= 5 \text{ pphm} \\ CO &= 10 \text{ ppm} \end{aligned}$$

and rate constants typical of those used in simulation studies of the Los Angeles airshed, we found that, after two hours, paired sets of results agreed to within 2% for all species. Our results were obtained using a four-minute time step and a relative error tolerance of 1%, while the results from the Gear routine were obtained using a one-minute time step.

To determine the effect that the size of the integration time step has on the predicted concentrations, we performed two simulations, identical in all respects except for the size of the time step. We chose the time period 1100-1300 PST since the photolysis rate constants are largest at this time of day. We carried out a normal simulation starting at 0500 PST and terminated it at 1100 PST. We then used the results obtained at 1100 PST as the initial conditions for the test. The two integrations were performed using one-minute and four-minute time steps. For purposes of comparison we calculated the percentage difference between the two results in each grid cell at 1300 PST,

$$\% \text{ Difference} = \left| \frac{C^* - C^{**}}{C^*} \right| \times 100\%$$

where C^* = result using a 1-minute time step

C^{**} = result using a 4-minute time step.

We then averaged the percentage differences in all grid cells and also found the largest percentage difference. The results are presented below:

Species	Average % Difference	Largest % Difference
RHC	0.9	3.1
NO	2.2	6.9
O_3	1.8	6.3
NO_2	1.4	2.1
CO	0.8	4.9
URHC	0.6	2.9

Based on these results, we adopted a four-minute maximum time step. In some instances, however, it is necessary to reduce the size of the time step. For example, if a negative concentration is ever predicted, then the size of the time step is decreased, and the integration sequence is reinitiated. We note that negative numbers may be predicted by the horizontal advection scheme if the time step is too large. The time step size is also reduced whenever the iterative procedure in Step III fails to converge in a reasonable number of iterations (say 20). The relative error tolerance was chosen as 0.01 to insure that the Newton iterative process had converged, or at least that the concentrations were not changing by more than one percent.

The final observation to be made with regard to the numerical scheme deals with the order in which Equations (21) - (23) are processed computationally. We note that there is no particular reason to integrate in the ξ direction first; in fact, it is just as reasonable to integrate in the η direction first. To reduce the possibility of introducing a bias into the predictions that might result from employing a fixed integration sequence, we apply the following rule regarding the order in which Equations (21) - (23) are integrated:

	Computational Order		
	Step I	Step II	Step III
odd-numbered time steps:	ξ - direction	η - direction	ρ - direction
even-numbered time steps:	η - direction	ξ - direction	ρ - direction

Thus the integration sequence is ξ-η-ρ, η-ξ-ρ, ξ-η-ρ, and etc. In Section I, we give the algorithm for the ξ-η-ρ sequence. The algorithm for the η-ξ-ρ sequence differs from the ξ-η-ρ sequence only in that values of

$$_{\ell}C^{*}_{i,j,k}$$

are determined from the finite-difference representation of Equation (22), and values of

$$_{\ell}C^{**}_{i,j,k}$$

are determined from the finite-difference approximation of Equation (21).

REFERENCES

Conte, S. D., "Elementary Numerical Analysis," McGraw-Hill, New York (1965).

Crowley, W. P., Monthly Weather Review, 96, 1 (1968).

Fromm, J. C., Physics of Fluids Supplement II, II-3 (1969).

Gear, C. W., Communications of the ACM, 14, 176 (1971).

Isaacson E., Keller, H. B., "Analysis of Numerical Methods," John Wiley & Sons, New York (1966).

Price, H. S., Varga, R. S., Warren, J.E., Journal of Math. Physics, 45, 301 (1966).

Roth, P. M., Reynolds, S. D., Roberts, P. J. W., Seinfeld, J. H., Development of a Simulation Model for Estimating Ground Level Concentrations of Photochemical Pollutants, Final Report and 6 Appendices, Systems Applications, Inc., Beverly Hills, California (1971).

Yanenko, N. N., "The Method of Fractional Steps," Springer-Verlag, New York (1971).